

# Anomalous critical behavior near the quantum critical point of a hole-doped $\text{La}_2\text{CuO}_4$

Y. Chen,<sup>1</sup> Wei Bao,<sup>1</sup> J.E. Lorenzo,<sup>2</sup> A. Stunault,<sup>3</sup> J.L. Sarrao,<sup>1</sup> S. Park,<sup>4,5,6</sup> and Y. Qiu<sup>4,5</sup>

<sup>1</sup>Los Alamos National Laboratory, Los Alamos, NM 87545

<sup>2</sup>CNRS, BP 166X, F-38043, Grenoble, France

<sup>3</sup>Institut Laue-Langevin, BP 156, F-38042, Grenoble, France

<sup>4</sup>NIST Center for Neutron Research, National Institute of Standards and Technology, Gaithersburg, MD 20899

<sup>5</sup>Dept. of Materials Science and Engineering, University of Maryland, College Park, MD 20742

<sup>6</sup>HANARO Center, Korea Atomic Energy Research Institute, Daejeon 305-600, Korea

(Dated: October 28, 2018)

The Landau-Ginzburg-Wilson paradigm for critical phenomena is spectacularly successful whenever the critical temperature is finite and all fluctuation modes, with characteristic energies much smaller than  $k_B T_C$ , obey classical statistics. In zero-temperature quantum critical phenomena, classical thermal fluctuations are replaced by zero-point quantum fluctuations and quantum-mechanical generalization of the Landau-Ginzburg-Wilson paradigm has been a central topic in condensed-matter physics. In this neutron-scattering study on spin fluctuations near the quantum critical point induced by hole-doping in  $\text{La}_2\text{Cu}_{1-x}\text{Li}_x\text{O}_4$  ( $0.04 \leq x \leq 0.1$ ), the phase boundary for quantum crossover expected from the generalized quantum theory for critical phenomena was observed for the first time. Furthermore, critical exponent and scaling function become anomalous near the quantum critical point, which has not been expected in current theories.

Interesting phenomena, including high- $T_C$  superconductivity, occur in laminar cuprates below a temperature  $T \ll J/k_B \approx 1500$  K, where  $J$  is the magnetic exchange energy between the nearest-neighbor spins in the  $\text{CuO}_2$  plane. In this temperature range, quantum fluctuations become dominant and add one extra dimension,  $\xi_T \equiv \hbar c/k_B T$ , where  $c$  is the spin-wave velocity, to the 2-dimensional (2D)  $\text{CuO}_2$  square lattice[1, 2] (Fig. 1). At the zero temperature, a quantum phase transition from the antiferromagnetic (AF) phase to a paramagnetic one occurs at a critical hole doping, a.k.a. quantum critical point (QCP),  $x_c$ , in the cuprates. Thus, for doping  $x > x_c$  on the paramagnetic side of the QCP, magnetic correlation length at  $T = 0$ ,  $\xi_0$ , is finite. Generalizing the Landau-Ginzburg-Wilson paradigm for critical phenomena in classical systems to the quantum spin system in the (2+1)-dimensional space, the shorter of  $\xi_T$  and  $\xi_0$  sets the long-wavelength cutoff for spin fluctuations and is expected to determine the universal magnetic phenomena with universal critical exponents[3]. The  $E/T$  scaling in spin dynamics, observed in diverse samples of hole-doped  $\text{La}_2\text{CuO}_4$  using Ba, Sr or Li dopant, with superconducting or insulating ground state, and with commensurate or incommensurate dynamic spin correlations[4, 5, 6, 7], can be understood as the physical consequence of  $\xi_T < \xi_0$  at  $T > T_X \equiv \hbar c/k_B \xi_0$ .

In this neutron scattering study on quantum spin dynamics in hole-doped  $\text{La}_2\text{CuO}_4$ , we determine the doping dependence of the crossover temperature  $T_X$ , below which the  $E/T$  scaling breaks down and crosses over to a constant-energy scaling, consistent with  $\xi_0 < \xi_T$ . The most interesting result of this study, however, is that the critical exponent  $a$  in the  $E/T$  scaling[3] changes from an expected  $a \approx 1$  to an anomalous  $a \approx 0.65$  when doping is reduced toward the AF QCP at  $x_c$ . The change of the

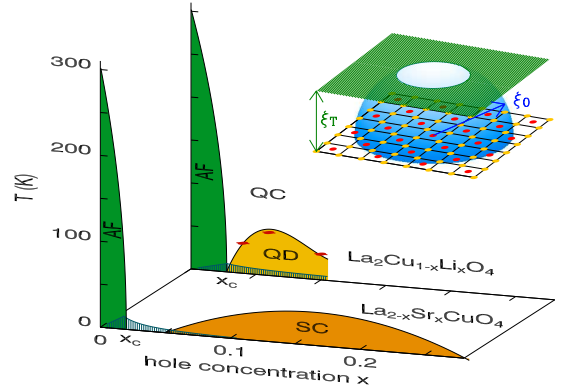


FIG. 1: (color) Phase diagrams for Sr and Li-doped  $\text{La}_2\text{CuO}_4$  where increasing hole concentration suppresses the antiferromagnetic (AF) phase at the quantum critical point  $x_c$  and drives the Sr doped material superconducting (SC). The line filled area denotes spin-glass phase. We observe the crossover at  $T_X$  (red symbols) between the  $E/T$  scaling (QC) and the  $E/\Gamma_0$  scaling (QD) regimes in Li-doped  $\text{La}_2\text{CuO}_4$ . The inset illustrates the (2+1)-dimensional space formed by the  $\text{CuO}_2$  plane (Cu: red circles, O: yellow circles) and the quantum  $\xi_T$ . The blue hemisphere indicates the extent of the magnetic correlation length at zero temperature,  $\xi_0$ .

critical exponent is inconsistent with the classical universality of critical exponents. In analog to a recent example in heavy fermion metal[8, 9], the substantial reduction of the  $a$  exponent in the 2D spin system suggests extra physics in quantum critical phenomena which invalidates the classical Landau-Ginzburg-Wilson paradigm[10].

We choose Li-doped  $\text{La}_2\text{CuO}_4$  single crystals for this study (Table I). Isotopically enriched  $^7\text{Li}$  (98.4%) was used to reduce neutron absorption of natural Li. The crystals have orthorhombic  $Cmca$  symmetry in the tem-

TABLE I: Doping  $x$  of  $\text{La}_2\text{Cu}_{1-x}\text{Li}_x\text{O}_4$  and main experimental quantities determined in this study

| $x$       | 0.04            | 0.06            | 0.1             |
|-----------|-----------------|-----------------|-----------------|
| $T_X$ (K) | 35              | 50              | 30              |
| $a$       | $0.65 \pm 0.06$ | $\approx 1$     | $\approx 1$     |
| $b$       | $0.21 \pm 0.01$ | $0.18 \pm 0.01$ | $0.28 \pm 0.01$ |

perature range of this study and lattice parameters were reported in [11]. Analogous to Sr-doped  $\text{La}_2\text{CuO}_4$ [12, 13, 14], the AF phase is suppressed rapidly by 3 percent of holes and a spin-glass transition occurs below 10 K on both sides of the QCP[15, 16] (Fig. 1). In addition, similar spin dynamics following the  $E/T$  scaling have been observed[4, 5, 6, 7]. To investigate the intrinsic spin dynamics of the 2D quantum antiferromagnet, the suppression of the  $d$ -wave superconductivity by Li dopants as potential scatterers in the  $\text{CuO}_2$  plane[17] is crucial. This allows measurement of the momentum and energy-dependent dynamic magnetic structure factor,  $S(\mathbf{q}, E)$ , at low temperature without interference by the superconducting gap as seen in Sr or Ba-doped  $\text{La}_2\text{CuO}_4$ [18, 19]. To achieve required energy resolution, the cold neutron triple-axis spectrometer IN14 at the Institut Laue-Langevin with  $E_f=5$  meV (for  $x=0.1$ ), and SPINS at the National Institute of Standards and Technology Center for Neutron Research with  $E_f=3.7$  meV (for  $x=0.04$ ) were used. The scattered neutron beam was filtered using cooled Be or BeO to remove higher order neutrons. The dynamic spin correlations which can be resolved in this cold neutron inelastic scattering study do not participate in the spin-freezing process[7]. We will report the minority spin-glass phase elsewhere.

Dynamic spin correlations in Li-doped  $\text{La}_2\text{CuO}_4$  are finite-sized fluctuating versions of the chessboard-like antiferromagnetic order in pure  $\text{La}_2\text{CuO}_4$ [20]. Intensity of  $S(\mathbf{q}, E)$  concentrates in reciprocal space in rods intercepting the planar Brillouin zone of the  $\text{CuO}_2$  square lattice at commensurate Bragg points of the  $(\pi, \pi)$ -type. Scans at various  $E$  and  $T$  across the rod at  $\mathbf{Q} \equiv (\pi, \pi)$  are shown in the inset to Fig. 2 for Li doping  $x=0.1$ . Note that  $\mathbf{Q}=(100)$  in the orthorhombic notation. The scans have been normalized by the peak intensities so that the invariance of the in-plane peak width in this work using coarse  $\mathbf{q}$  resolution can be easily seen. Reflecting the two-dimensional nature of spin correlations,  $S(\mathbf{q}, E)$  is flat in the out-of-plane direction[7]. Thus,  $\int d\mathbf{q} S(\mathbf{q}, E)$  is simply proportional to the value of  $S(\mathbf{Q}, E)$  in the  $T$  and  $E$  range of this study, and the imaginary part of the local magnetic response function  $\chi''(E) \equiv (1 - e^{-E/k_B T}) \int d\mathbf{q} S(\mathbf{q}, E)$  is proportional to  $(1 - e^{-E/k_B T}) S(\mathbf{Q}, E)$ . Measured  $S(\mathbf{Q}, E)$  as a function of  $E$  and  $T$  is shown in Fig. 2a and b for  $x=0.1$  and 0.04, respectively. Throughout this paper, a unique

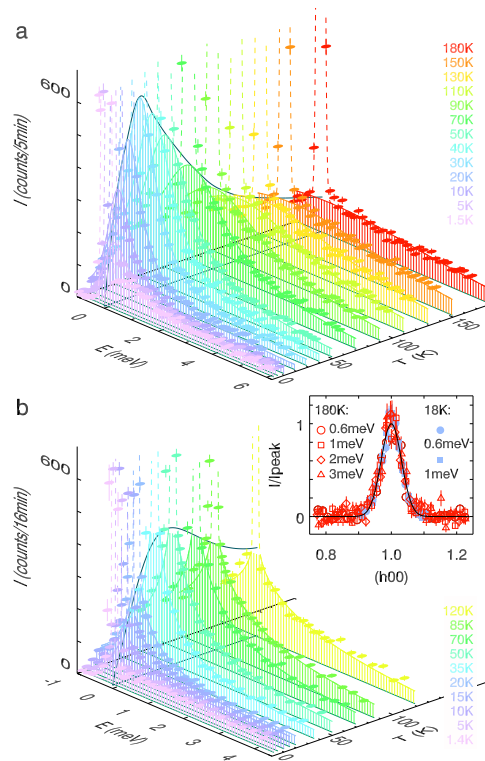


FIG. 2: (color) Measured dynamic magnetic structure factor  $S(\mathbf{Q}, E)$  as a function of  $E$  and  $T$  at  $\mathbf{Q}=(100)$  in the  $Cmca$  orthorhombic notation which corresponds to the  $(\pi, \pi)$  point of the  $\text{CuO}_2$  square lattice. **a**, Li doping  $x=0.1$ . **b**,  $x=0.04$ . The blue curve at  $E=0$  traces  $S(\mathbf{Q}, E)$  at the low energy limit as a function of temperature. Inset: normalized  $S(\mathbf{q}, E)$  as a function of  $\mathbf{q}$  at indicated  $E$  and  $T$  for  $x=0.1$ .

color is assigned to each temperature for data points in the figures. The peak at  $E=0$  (dashed curves) contains incoherent, elastic and quasielastic scattering processes within the energy resolution,  $\Delta_{\text{res}}$ , of the spectrometer and is not the subject of this work. For the resolvable dynamic signal,  $S(\mathbf{q}, E)$  with  $|E| > \Delta_{\text{res}}$ , background (straight green lines) is determined by measurement at  $\mathbf{q}$  far away from the peak of  $S(\mathbf{q}, E)$  (refer to the inset to Fig. 2), or at  $E \ll -k_B T$  where the Bose factor for spin fluctuation modes approaches zero.

To demonstrate the  $E/T$  scaling in magnetic response function:

$$\chi''(E)T^a = Af(E/bk_B T), \quad (1)$$

where  $a$  is a critical exponent[3],  $A$  a constant,  $f(y)$  a scaling function defined to peak at  $y=1$ , and  $b = E_p/k_B T$  relates the peak energy of  $\chi''(E)$  to thermal energy, experimental data of  $\chi''(E)$  above  $T_X$ , renormalized by  $T^{-a}$ , are plotted semilogarithmically as a function of  $E/k_B T$  for  $x=0.1$  and 0.04 in Fig. 3a and b, respectively.

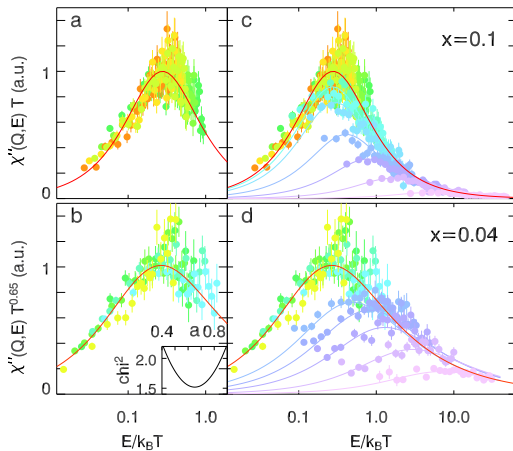


FIG. 3: (color) Scaling plots of the magnetic response function. **a, b**, The  $E/T$  scaling at high temperature for  $x=0.1$  and  $0.04$ , respectively. Inset in **b** shows the goodness-of-fit for the critical exponent  $a=0.65$  for  $x=0.04$ . **c, d**, Departure from the  $E/T$  scaling at low temperature. The solid line in **a** and **c** is Eq. (1) using Eq. (2) as the scaling function, in **b** and **d** using Eq. (3) as the scaling function. Color of symbols denotes temperature as in Fig. 2.

For  $x=0.1$ , identical to the case for  $x=0.06$ [7],  $a \approx 1$  and the scaling function is

$$f_1(y) = y/(1 + y^2). \quad (2)$$

The peak position  $E_p/k_B T = b = 0.28 \pm 0.01$  in Fig. 3a is larger than  $b=0.18$  for  $x=0.06$ . For Ba or Sr-doped  $\text{La}_2\text{CuO}_4$ , the exponent  $a$  has been determined only for  $x=0.14$  and it is also  $a = 0.94 \pm 0.06 \approx 1$ [6]. Thus for  $x \geq 0.06$ , hole-doped  $\text{La}_2\text{CuO}_4$  has a normal critical exponent  $a \approx 1$ , consistent with a Curie's law for the staggered magnetic susceptibility.

For Li doping  $x=0.04$  which is close to the AF QCP of  $x_c \approx 0.03$ [11], a fractional  $a=0.65 \pm 0.06$  is required for the data to collapse onto a single scaling curve (Fig. 3b). Previously, in heavy fermion alloy  $\text{CeCu}_{5.9}\text{Au}_{0.1}$ , which is also near an AF QCP, single-crystal neutron scattering data are collapsed onto the  $E/T$  scaling with  $a=0.74 \pm 0.1$ [8]. The same procedure as in Ref. [8], which is unbiased with respect to the selection of  $f(y)$ , is used to optimize  $a$  for  $x=0.04$ , and the goodness-of-fit represented by the chi-square statistical test is shown in the inset to Fig. 3b. The spectrum in Fig. 3b is broader than that in Fig. 3a and cannot be described by Eq. (2). We adopt empirically the scaling function for  $x=0.04$ ,

$$f_2(y) = \text{sgn}(y) y_1^u / (1 + y_1^v), \quad (3)$$

where  $y_1 \equiv |y|[(v - u)/u]^{1/v}$  with  $u=0.77 \pm 0.02$  and  $v=1.33 \pm 0.02$  as the best fits. The parameter  $b = 0.21 \pm 0.01$ . Note that for  $|y| \ll 1$ ,  $f_2(y) \sim \text{sgn}(y)|y|^u$  is also anomalous and does not conform to the usual analytic form  $\chi''(E) \sim E$  at small  $E$ [3].

The heavy fermion metal  $\text{CeCu}_{5.9}\text{Au}_{0.1}$  ( $z=2$  and dimension  $d > 2$ ) and our  $x=0.04$  cuprate sample ( $z=1$  and  $d=2$ ) belong to different universality classes with the effective dimension ( $d+z$ ) above and below the upper critical dimension, respectively[1, 21]. However, they are both close to an AF QCP and share within error bars an anomalous  $a$  exponent substantially smaller than unity. In our study of doping dependence, furthermore, hole-doped  $\text{La}_2\text{CuO}_4$  recovers the normal  $a \approx 1$  and analytic  $\chi''(E)$  for  $x \geq 0.06$ . These changes in critical behavior are very unusual. Anomalous  $a$  exponent for the heavy fermion metal  $\text{CeCu}_{5.9}\text{Au}_{0.1}$  is recently explained by including local degrees of freedom in the Kondo screening, in addition to traditional long-wavelength magnetic fluctuations, in the antiferromagnetic quantum phase transition[9]. Closer to our case of doped cuprates near the AF QCP, currently, “deconfined” degrees of freedom associated with fractionalization of magnetic order parameter in pure 2D antiferromagnet are being explored theoretically[10]. Like Ref. [9], this theory goes beyond the Landau-Ginzburg-Wilson paradigm, which focuses on long-wavelength fluctuations of the order parameter in critical phenomena. Whether including these additional “deconfined” degrees of freedom in the critical theory for the QCP would, similar to the case for heavy fermion metals[9], produce the anomalous  $a$  exponent and  $f_2(y)$  reported here for cuprates is unknown. Nevertheless, our observation of anomalous critical phenomena near the QCP in another class of correlated electronic material suggests the generality of the phenomena, and would certainly encourage the budding research interest on subtle quantum interference effects near a QCP.

In Fig. 3c and d, low temperature data are added to the scaling plots for  $x=0.1$  and  $0.04$ , respectively. Since the peak position shifts to the right with decreasing temperature, the  $E/T$  scaling cannot be satisfied. Instead, as shown in Fig. 4a and b, below  $T_X$ , the local magnetic response function  $\chi''(E)$  is nearly temperature independent. The curves in the figures are

$$\chi''(E) = Bf(E/\Gamma_0), \quad (4)$$

where  $B$  is a constant, and the same pair of scaling functions,  $f_1(y)$  and  $f_2(y)$ , are used in Eq. (4) with  $\Gamma_0=0.66 \pm 0.01$  and  $1.11 \pm 0.03$  meV for  $x=0.1$  and  $0.04$ , respectively. Note that there is no detectable gap in  $\chi''(E)$  in Fig. 4 for  $x=0.1$  and  $0.04$ , as for  $x=0.06$  reported previously[7]. In some theoretical models of non-random quantum antiferromagnets, a quantum spin liquid has a gap,  $\Delta \sim \hbar c/\xi_0$ , near  $E=0$  in  $\chi''(E)$  below  $T_X$ [21]. The gapless  $\chi''(E)$  observed in our samples is obtained in these theories with strong damping of the spin liquid by doped holes,  $\Gamma \approx \Delta$ [22, 23]. Partial filling of the Haldane gap in 1D quantum spin liquid by doped holes has been reported lately[24]. In other theoretical models of quantum antiferromagnets, several types of gapless spin liquids exist without impurity scattering[25]. Clas-

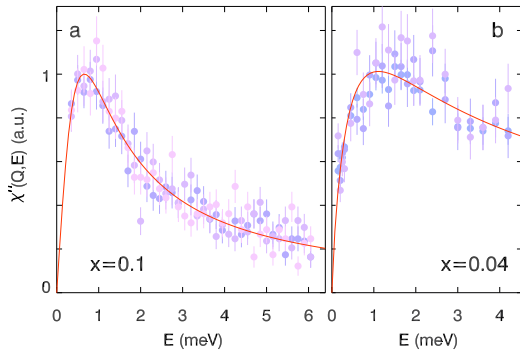


FIG. 4: (color) Temperature invariance of the magnetic response function at  $T < T_X$ . **a**, The doping  $x=0.1$ . The solid line is Eq. (4) using Eq. (2) as the scaling function. **b**,  $x=0.04$ . The solid line is Eq. (4) using Eq. (3) as the scaling function. Color of symbols denotes temperature as in Fig. 2.

sification of our observed 2D gapless spin liquid in hole-doped cuprates would be an interesting theoretical task.

The crossover temperature,  $T_X$ , from the  $E/T$  scaling to the  $E/\Gamma_0$  scaling regime can be conveniently located by the peak in temperature dependence of  $S(\mathbf{Q}, E)$  at the  $E \rightarrow 0$  limit[7], since at high temperature,  $S(\mathbf{Q}, E \rightarrow 0) \propto T^{-a}$  from Eq. (1)-(3), and at low temperature  $S(\mathbf{Q}, E \rightarrow 0) \propto T$  from Eq. (2)-(4). The blue curves at  $E=0$  in Fig. 2a and b are  $S(\mathbf{Q}, E \rightarrow 0)$  for  $x=0.1$  and 0.04, respectively. The extracted  $T_X$  from Fig. 2, together with previously determined value for  $x=0.06$ [7], are shown in the phase diagram in Fig. 1 and are listed in Table I. Under the dome-shaped phase boundary, spin fluctuation energy, which would approach zero according to the  $E/T$  scaling, saturates at a finite  $\Gamma_0$ . Thus the crossover at  $T_X$  keeps spin fluctuations energetic at low temperature, which might be essential for the high value of  $T_C$  if superconductivity in cuprates is mediated magnetically by spin fluctuations.

Experimental search for the  $E/T$  scaling was initially stimulated by the marginal Fermi liquid phenomenology[4, 5, 26]. The subsequent observation of the scaling in insulating sample[7] supports the QCP as the common mechanism. The breakdown of the  $E/T$  scaling below a dome-shaped crossover boundary reported here excludes the existence of additional magnetic QCPs in the investigated doping range. The gapped quantum spin liquid predicted below  $T_X$  for non-random 2D antiferromagnets does not survive in our doped cuprates. This observation disfavors those theories which rely on the robustness of the gapped quantum spin liquid against doping for high- $T_C$  superconductivity in cuprates[27]. While the application of the classical Landau-Ginzburg-Wilson paradigm for critical phe-

nomena to quantum critical phenomena in cuprates naturally explains the universal occurrence of the  $E/T$  scaling in hole-doped  $\text{La}_2\text{CuO}_4$  and the crossover to the finite magnetic-energy regime at low temperature[2, 3], the anomalous critical exponent and scaling function near the QCP reported here have yet to be understood, probably by going beyond the Landau-Ginzburg-Wilson paradigm and taking into account additional quantum interference effects existing near the zero temperature[9, 10].

We thank Q.M. Si, A. Zheludev, S.-H. Lee, C. Broholm, S. Sachdev, A.V. Chubukov, F.C. Zhang, C.M. Varma, X.G. Wen, A. Balatsky, A. Abanov, L. Yu, Z.Y. Weng and Y. Bang for useful discussions. SPINS at NIST is supported partially by NSF. Work at LANL is supported by U.S. Department of Energy.

- 
- [1] J. A. Hertz, *Phys. Rev. B* **14**, 1165 (1976); A. J. Millis, *ibid.* **48**, 7183 (1993).
  - [2] S. Chakravarty, B. I. Halperin, and D. R. Nelson, *Phys. Rev. Lett.* **60**, 1057 (1988).
  - [3] S. Sachdev and J. Ye, *Phys. Rev. Lett.* **69**, 2411 (1992).
  - [4] S. M. Hayden, *et al.*, *Phys. Rev. Lett.* **66**, 821 (1991).
  - [5] B. Keimer, *et al.*, *Phys. Rev. Lett.* **67**, 1930 (1991).
  - [6] G. Aeppli, T. E. Mason, S. M. Hayden, H. A. Mook, and J. Kulda, *Science* **278**, 1432 (1997).
  - [7] W. Bao, Y. Chen, Y. Qiu, and J. L. Sarrao, *Phys. Rev. Lett.* **91**, 127005 (2003).
  - [8] A. Schröder, G. Aeppli, E. Bucher, R. Ramazashvili, and P. Coleman, *Phys. Rev. Lett.* **80**, 5623 (1998).
  - [9] Q. M. Si, *et al.*, *Nature* **413**, 804 (2001).
  - [10] T. Senthil, *et al.*, *Science* **303**, 1490 (2004).
  - [11] J. L. Sarrao, *et al.*, *Phys. Rev. B* **54**, 12014 (1996).
  - [12] F. C. Chou, *et al.*, *Phys. Rev. Lett.* **71**, 2323 (1993).
  - [13] T. Nagano, *et al.*, *Phys. Rev. B* **48**, 9689 (1993).
  - [14] C. Niedermayer, *et al.*, *Phys. Rev. Lett.* **80**, 3843 (1998).
  - [15] R. H. Heffner, D. E. MacLaughlin, G. J. Nieuwenhuys, J. L. Sarrao, and J. E. Sonier, *Physica B* **312**, 65 (2002).
  - [16] T. Sasagawa, *et al.*, *Phys. Rev. B* **66**, 184512 (2002).
  - [17] P. A. Lee, *Phys. Rev. Lett.* **71**, 1887 (1993).
  - [18] T. E. Mason, G. Aeppli, S. M. Hayden, A. P. Ramirez, and H. A. Mook, *Phys. Rev. Lett.* **71**, 919 (1993).
  - [19] K. Yamada, *et al.*, *Phys. Rev. Lett.* **75**, 1626 (1995).
  - [20] W. Bao, *et al.*, *Phys. Rev. Lett.* **84**, 3978 (2000).
  - [21] S. Sachdev, *Quantum Phase Transitions* (Cambridge University Press, Cambridge, 1999).
  - [22] S. Sachdev, A. V. Chubukov, and A. Sokol, *Phys. Rev. B* **51**, 14874 (1995).
  - [23] Y. L. Liu and Z. B. Su, *Phys. Lett. A* **200**, 393 (1995).
  - [24] G. Xu, *et al.*, *Science* **289**, 419 (2000).
  - [25] X. G. Wen, *Phys. Rev. B* **65**, 165113 (2002).
  - [26] C. M. Varma, P. B. Littlewood, S. Schmitt-Rink, E. Abrahams, and A. E. Ruckenstein, *Phys. Rev. Lett.* **63**, 1996 (1989).
  - [27] S. Sachdev, *Science* **288**, 475 (2000).